HHS Public Access

Author manuscript

Cell Oncol (Dordr). Author manuscript; available in PMC 2016 June 09.

Published in final edited form as:

Cell Oncol (Dordr). 2016 June ; 39(3): 265–277. doi:10.1007/s13402-016-0272-x.

A novel curcumin-like dienone induces apoptosis in triple-negative breast cancer cells

Elisa Robles-Escajeda[1], **Umashankar Das**[2], **Nora M. Ortega**[1], **Karla Parra**[1], **Giulio Francia**[1], **Jonathan R. Dimmock**[2], **Armando Varela-Ramirez**[1], and **Renato J. Aguilera**[1]

[1] Cytometry, Screening and Imaging Core Facility, Border Biomedical Research Center, Department of Biological Sciences, the University of Texas at El Paso, 500 West University Avenue, El Paso, TX 79968-0519, USA

[2] Drug Discovery & Development Research Group, College of Pharmacy & Nutrition, University of Saskatchewan, 110 Science Place, Saskatoon, SK S7N 5C9, Canada

Abstract

Purpose—According to the World Health Organization (WHO), breast cancer is the most common cancer affecting women worldwide. In the USA ~12.3 % of all women are expected to be diagnosed with various types of breast cancer, exhibiting varying degrees of therapeutic response rates. Therefore, the identification of novel anti-breast cancer drugs is of paramount importance.

Methods—The 1,5-diaryl-3-oxo-1,4-pentadienyl pharmacophore was incorporated into a number of cytotoxins. Three of the resulting dienones, 2a, 2b and 2c, were tested for their antineoplastic potencies in a variety of human breast cancer-derived cell lines, including the triple negative MDA-MB-231 cell line and its metastatic variant, using a live-cell bio-imaging method. Special emphasis was put on dienone 2c, since its anti-cancer activity and its mode of inflicting cell death have so far not been reported.

Results—We found that all three dienones exhibited potent cytotoxicities towards the breast cancer-derived cell lines tested, whereas significantly lower toxicities were observed towards the non-cancerous human breast cell line MCF-10A. The dienones 2b and 2c exhibited the greatest selective cytotoxicity at submicromolar concentration levels. We found that these two dienones induced phosphatidylserine externalization in MDA-MB-231 cells in a concentration-dependent manner, suggesting that their cytotoxic effect might be mediated by apoptosis. This possibility was confirmed by our observation that the dienone 2c can induce mitochondrial depolarization, caspase-3 activation, cell cycle disruption and DNA fragmentation in MDA-MB-231 cells.

Conclusion—Our findings indicate that dienone 2c uses the mitochondrial/intrinsic pathway to inflict apoptosis in triple negative MDA-MB-231 breast cancer-derived cells. This observation warrants further assessment of dienone 2c as a potential anti-breast cancer drug.

Armando Varela-Ramirez, avarela2@utep.edu. Renato J. Aguilera, raguilera@utep.edu.

Compliance with Ethical Standards

Conflict of Interest The authors declare no conflict of interest.

Keywords

Anti-cancer drug discovery; Apoptosis; Caspase-3; Cell cycle; DNA fragmentation; Mitochondrial depolarization; Curcumin analogues

1 Introduction

Carcinoma of the breast is the most frequently diagnosed tumor type and a common cause of cancer-related death in women worldwide. In the USA alone, around 40,290 women are predicted to die from breast cancer in 2015, while the worldwide death rate will approximate 450,000 cases [1]. It has also been estimated that in the USA during 2015, 231,840 new cases of invasive breast cancer will be diagnosed. Recurrent and metastatic breast cancers are the main causes of death [2]. Around 12.3 % of women in the USA are expected to be diagnosed with some type of breast cancer during their lifetime [1, 3]. Based on these alarming statistics, the identification of novel anti-breast cancer drugs is considered to be of paramount importance.

Human breast cancer encompasses a diverse group of malignancies with distinct characteristics concerning their clinical evolution, genotype, phenotype, response to therapy and prognosis [3–7]. One subgroup of breast cancers comprises cells lacking expression of the estrogen receptor (ER), the progesterone receptor (PR) and the human epidermal growth factor receptor 2 (HER2) [3, 8]. These so called triple-negative breast cancers belong to the most aggressive and therapy-resistant tumors [9]. Triple-negative breast cancers have also been associated with the occurrence of lymph node metastases and an unfavorable survival [10]. In the current report, novel dienone curcumin-like derivatives were tested on different human breast cancer-derived cell types, ranging from ER^+, PR^+, $HER2^+$ to hormone-independent triple-negative MDA-MB-231 cells [11] and its metastatic variant MDA-MB-231/LM2-4 [12]. A prominent challenge in cancer chemotherapy is the development of drugs displaying a selective toxicity towards cancer cells. Therefore, we also included MCF-10A cells, which are derived from human non-cancerous breast epithelial tissue [13], to determine the degree of selective cytotoxicity. In the anti-cancer drug discovery context, the selective cytotoxicity index (SCI) is defined as the ability of an experimental drug to preferentially kill cancer cells, without harming non-cancerous cells under similar conditions (modified from Robles-Escajeda [14]).

Curcumin, 1,7-bis(4-hydroxy-3-methoxyphenyl)-1,6-heptadiene-3,5-dione, also known as diferuloylmethane, is an α,β-diketone natural polyphenol compound and active ingredient of turmeric condiment derived from *Curcuma longa*. In the past, curcumin has been found to exhibit anti-inflammatory, anti-proliferative and anti-cancer activities [15–17]. For a number of years, various curcumin analogues, i.e., conjugated and unsaturated ketones, have been designed as antineoplastic thiol alkylating agents. These analogues have the capacity to react with thiols while interactions with amines and hydroxyl groups, which are present in nucleic acids, are minute or non-existent [18]. Hence, these analogues may be devoid of the genotoxic properties of other contemporary anticancer agents [19]. In addition, the curcumin analogues 1,5-diaryl-3-oxo-1,4-pentadienes [20], referred to as dienones, are known to

exhibit interactions with cellular thiols that can be sequential, i.e., initially at one olefinic carbon atom and subsequently at a second one. This sequence of events may lead to tumor-selective toxicity, since various studies have shown that when an initial chemical insult is followed by a second toxic interaction, some tumor cells become more sensitive to this type of drugs than normal cells [21, 22]. These considerations led to the preparation of dienone series 1 (Fig. 1a), which was found to exhibit anti-neoplastic properties towards various leukemia and lymphoma cells [23]. Based on these preliminary findings, it was decided to attach an acyl group onto the piperidyl nitrogen atom leading to dienone series 2 (Fig. 1a), which may allow binding to additional cellular constituents. In many cases, the potency of the dienones in series 2 increased compared to those in series 1, which bore the same substituents in the arylidene aryl rings A and B [24].

Here, we tested the cytotoxic properties of three curcumin analogues, designated dienones 2a-c, whose structures are presented in Fig. 1. The CC_{50} values were determined using a live-cell assay [25] in four human breast cancer-derived cell lines and one non-malignant breast epithelial-derived cell line. In addition, 5-fluorouracil (5-FU), which is currently utilized for the management of breast cancer, was used to compare its activity with the novel dienones. Subsequently, dienone 2c was selected for further analysis to distinguish between apoptosis and necrosis in MDA-MB-231 breast cancer-derived cells by assessing their capacity to evoke plasma membrane phosphatidylserine (PS) translocation, mitochondrial depolarization, caspase-3 activation and DNA fragmentation. Our results indicate that dienone 2c preferentially induces apoptosis in these triple-negative breast cancer cells.

2 Materials and methods

2.1 Curcumin analogues

The synthesis of dienones 2a (3,5-bis(benzylidene)-1-[4-(2-diethylaminoethyloxy) phenylcarbonyl]-4-piperidone hydrochloride hemihydrate) and 2b (1-[4-(2-dimethylaminoetho xy)phen y lcarbony l]-3 ,5-bis(4-methylbenzylidene)-4-piperidone hydrochloride hemihydrate) has been reported before [24], whereas the synthesis of dienone 2c (3,5-bis(benzylidene)-1-[3-(2-dimethylaminoethoxy) phenylcarbonyl]-4-piperidone hydrochloride), which was prepared in an analogous manner, will be reported elsewhere. The purity of the dienones was ascertained by 500 MHz ^{1}H NMR spectroscopy and elemental analyses. All stock solutions and their resultant dilutions were prepared in dimethyl sulfoxide (DMSO; Sigma-Aldrich, St Louis, MO, USA). As necessary, aliquots of dienones were added directly to 24- or 96-well plates containing cells cultured in growth medium (see below).

2.2 Cell lines and culture conditions

The triple-negative human breast cancer-derived cell line MDA-MB-231 (ATCC, Manassas, VA, USA), derived from a patient with an adenocarcinoma [11] and its lung metastatic (LM) variant MDA-MB-231/LM2-4 line [12] were grown under identical conditions in DMEM medium (HyClone, Logan UT, USA) supplemented with 10 % heat-inactivated fetal bovine serum (FBS: Hyclone), 100 U/ml penicillin and 100 μg/ml streptomycin (Life Technologies, Grand Island, NY, USA). The human breast adenocarcinoma cell line MCF-7, derived from

a pleural effusion (triple-positive), was also grown in DMEM medium as described above, while the invasive ductal carcinoma-derived cell line HCC1419 (ER- and PR-negative, HER2-positive) was cultured in RPMI-1640 medium with the same supplements as described above plus 2 mM L-glutamine (Hyclone). The non-cancerous immortalized human mammary epithelial-derived cell line MCF-10A was used as a control and grown as previously reported [26], with slight modifications: DMEM/F12 medium (Life Technologies) supplemented with 10 % FBS, 10 μg/ml recombinant human insulin (Sigma), 20 ng/ml epidermal growth factor (Peprotech, Rocky Hill, NJ, USA), 0.5 μg/ml hydrocortisone (Sigma), 2.5 mM L-glutamine (Life Technologies), 100 U/ml penicillin and 100 μg/ml streptomycin (Life Technologies). All cell lines were derived from female donors [27]. Cells growing exponentially till 60–75 % confluence were detached by trypsinization, counted and seeded into 24- and 96-well plates at densities of 50,000 or 10,000 cells in 1 ml or 200 μl culture medium per well, respectively. The incubation conditions were kept consistent at 37 °C in a humidified 5 % CO_2 atmosphere. To ensure high viability, cells were prepared as previously reported [25].

2.3 Differential nuclear staining assay

The toxicity of the experimental dienones was ascertained using the human breast cancer-derived lines mentioned above, as well as the non-cancerous human epithelial breast-derived cell line. Cell toxicity was monitored using a live-cell differential nuclear staining (DNS) bio-imaging assay [25]. Cells were seeded in 96-well plates and incubated overnight to allow adherence. Next, the cells were treated with experimental dienones for 72 h. Several controls were incorporated in each assay, including DMSO (0.4 % *v*/*v*) as solvent control, hydrogen peroxide (H_2O_2; 100 μM) as a positive control and untreated cells as a negative control. One hour before imaging, a mixture of two fluorescent nucleic acid intercalators, at a final concentration of 1 μg/ml each, were added to each well, i.e., propidium iodide (PI; red signal; MP Biomedicals, Solon, OH, USA) and Hoechst 33342 (Hoechst; blue signal; Invitrogen, Eugene, OR, USA). Hoechst readily crosses the plasma membranes of healthy and dead cells, providing an estimate of the total number of cells, whereas PI only stains the nuclei of cells with a compromised plasma membrane integrity, thus denoting the number of dead cells. The fluorescence signal from each individual fluorophore emitted by the cell nuclei was acquired in two separate channels according to the excitation/emission requirements of the respective dyes. Images were captured directly from tissue culture microplates utilizing a BD Pathway 855 bio-imaging system (BD Biosciences Rockville, MD, USA). To evaluate adequate numbers of regions of interest (ROIs; equivalent to the number of nuclei/cells), 2×2 montages from four adjacent image fields were captured per well using a 10× objective. Image acquisition and data analysis to determine the percentage of dead cells from each individual well were achieved using the BD AttoVision™ v1.6.2 software package (BD Biosciences). Experimental data points, as well as all controls, were assessed in triplicate. CC_{50} values were calculated based on a linear interpolation equation, using a range of serial dilutions as previously reported [28].

2.4 Selective cytotoxicity index assay

The selective cytotoxicity index (SCI) for each dienone was calculated as follow: SCI = CC_{50} of non-cancerous cells / CC_{50} of cancer cells. SCI refers to the ability of a drug to

efficiently kill cancer cells with minimal toxicity to non-cancerous cells. SCI values of 1 or less are indicative for lack of selective cytotoxicity of a compound to kill a cancer cell, whereas SCI values greater than 1 are indicative for selective toxicity of a compound towards cancer cells compared to non-cancerous cells. High SCI values are required for any potential anti-cancer drug.

2.5 Annexin V/PI assay

MDA-MB-231 cells were seeded in 24-well plates at a density of 50,000 cells/well in 1 ml culture medium. The plates were incubated overnight to allow cell attachment, after which the experimental dienones were added at various concentrations, followed by incubation for 48 h. For the flow cytometry assays, floating and trypsinized cells from each individual well were collected in a pre-chilled cytometric tube, washed and handled essentially as previously described [14]. Briefly, cells were labeled with a solution containing a mixture of annexin V-FITC and PI in 100 µl binding buffer (Beckman Coulter, Miami, FL, USA). After a 15 min incubation on ice in the dark, 300 µl ice-cold binding buffer was added to the cell suspension which was immediately examined by flow cytometry (Cytomics FC 500; Beckman Coulter). The following controls were utilized: cells treated with 100 µM etoposide as a positive control for apoptosis, cells treated with 0.4 % *v*/*v* DMSO as solvent control and untreated cells as a negative control. The total percentage of apoptotic cells was defined as the sum of both early and late stages of apoptosis (i.e., annexin V-FITC positive).

2.6 Mitochondrial membrane potential (ΔΨm) assay

MDA-MB-231 cells seeded in 24-well plates were exposed for 8 h [29] to 10 and 25 µM dienone 2c and subsequently stained with 2 µM 5,5′,6,6′-tetrachloro-1, 1′,3,3′-tetraethylbenzimidazolylcarbocyanine iodide (JC-1) fluorophore, following the manufacturer's instructions (MitoProbe; Life Technologies, Grand Island, NY, USA). Cells with intact polarized mitochondria permit JC-1 aggregation, which emits a red signal, whereas cells with depolarized mitochondria induce the formation of JC-1 monomers, which emit a green signal. Control solvent (0.4 % *v*/*v* DMSO) and untreated cells were analyzed in parallel. Data acquisition and analysis were achieved using CXP software (Beckman Coulter) and each data point was analyzed in triplicate.

2.7 Live-cell detection of intracellular caspase-3 activation

MDA-MB-231 cells were seeded in 24-well plates as described above and treated with dienone 2c for 8 h [29]. Next, cysteine-aspartic protease (caspase)-3 activation was detected using a fluorogenic NucView 488 Caspase-3/7 substrate for live cells, following the manufacturer's instructions (Biotium, Hayward, CA, USA). This substrate is permeable to cells with an intact plasma membrane and permits the detection of caspase-3 activation in live cells. Cells emitting a green fluorescent signal (denoting caspase-3 activation) were identified by flow cytometry (Cytomics FC500, Beckman Coulter). Control solvent (0.4 % *v*/*v* DMSO) and untreated cells were analyzed in parallel.

2.8 Cell cycle analysis by flow cytometry

MDA-MB-231 cells (asynchronous cultures in logarithmic growth phase) were exposed to dienone 2c at increasing doses, and concomitant changes in cell cycle profiles were determined by DNA content using a Gallios flow cytometer (Beckman Coulter, Miami, FL, USA). This flow cytometer is equipped with a solid state 405 nm violet laser capable of exciting the nucleic acid intercalator DAPI (4′,6-diamidino-2-phenylindole, dihydrochloride), which was used to label the DNA. Briefly, cells were seeded in 24-well plates as detailed above and treated with 1 μM or 3 μM dienone 2c for 48 h under standard culture conditions. The following controls were included in this series of experiments: 4 μM camptothecin (CPT) as a reference drug, 0.1 % and 0.3 % *v*/*v* DMSO solvent and untreated cells. After a 48 h incubation, floating cells were harvested in a flow cytometric tube and placed on ice. The remaining adherent cells were collected after detachment with 300 μl 0.25 % trypsin solution (Life Technologies) for 5 min at 37 °C [28]. Cells from each individual well (both detached and floating) were centrifuged at 263×g for 5 min. The resulting cell pellets were gently resuspended in 100 μl of fresh medium. Subsequently, 200 μl nuclear isolation medium (NIM)-DAPI solution (NPE Systems, Inc. Pembroke Pines, FL, USA and Beckman Coulter) was added to the cell suspensions, incubated for 3 min at room temperature in the dark and immediately analyzed by flow cytometry [30]. The NIM-DAPI reagent is a combination of NP-40 detergent and DAPI, which permeabilize the plasma membrane and stain DNA, respectively. Approximately, 10,000 events (cells) were collected using a Gallios flow cytometer and the cell cycle phase distributions were analyzed using Gallios CXP 9.1 software (Beckman Coulter).

2.9 Statistical analysis

Experiments were repeated at least three times and reported as the average of triplicates with the corresponding standard deviations. The statistical significance of differences between two experimental samples was performed by a two-tailed paired Student's *t*-tests. For two-group comparisons of independent samples a P value of < 0.05 was deemed significant.

3 Results

3.1 Dienones 2a-c exert preferential cytotoxicity to breast cancer-derived cells

The cytotoxic effects of the experimental compounds were quantified using a DNS assay (see materials and methods). In Fig. 2 representative images of live and dead cells used to quantify the percentage of experimental compound-mediated cytotoxicity in MDA-MB-231 cells are depicted. Untreated cells were used as a negative control (Fig. 2a). Cells treated with H_2O_2 (100 μM), which results in a significant increase of dead/PI-positive cells, show a magenta color due to co-localization of blue (Hoechst) and red (PI) signals (positive control; Fig. 2b). Cells treated with the dienone 2c (0.8 μM) were found to exhibit a pattern similar to that of the H_2O_2 treated cells (Fig. 2c).

Different human cell lines incubated for 72 h with experimental dienones were analyzed. The breast cancer-derived cell lines used were MDA-MB-231 (non-metastatic) and its derivative MDA-MB-231-LM2-4 (metastatic), MCF-7 and HCC1419 (see materials and methods). The non-cancerous human breast epithelial-derived cell line MCF10-A was

included as a control. The CC_{50} and SCI values for each dienone for the different cell lines are shown in Table 1. In the cancer-derived cells the dienones exhibited CC_{50} values that were in the nanomolar to low micromolar range (0.53 μM to 4.4 μM). Overall, the effect of the control drug 5-FU on the cancer-derived cells was weaker compared to the dienones, with the exception of the MCF-7 cells, which were more sensitive to this drug (CC_{50} = 1.7 μM; Table 1). However, the dienones were significantly more cytotoxic (SCI ranging from18 to 150) to all the breast cancer-derived cells tested compared to the non-malignant MCF-10A cells ($P < 0.001$; Table 1). Compound 2a exhibited the lowest SCI (45) on MDA-MB-231 cells compared to 2b (SCI = 111) and 2c (SCI = 90; Table 1). From these results, we conclude that the three dienones tested (2a–c) exert a preferential cytotoxicity to the breast cancer-derived cells, with a significantly lower cytotoxicity to non-malignant breast-derived cells. Due to the higher SCI values obtained with 2b and 2c, these two were selected for further analyses.

3.2 Dienones 2b and 2c induce phosphatidylserine translocation in MDA-MB-231 cells

Phosphatidylserine (PS), which is preferentially located at the inner side of the plasma membrane leaflet facing the cytosol, is translocated to the membrane outer leaflet in cells undergoing apoptosis. Annexin V (~36 kDa) has a high affinity for PS and, when conjugated to FITC, it allows an accurate detection of PS externalization by flow cytometry. In order to determine whether the observed cytotoxicity was exerted via apoptosis or necrosis, MDA-MB-231 cells were treated with several concentrations of the dienones 2b (1 and 5 μM) and 2c (5, 10 and 25 μM) for 48 h. We found that both dienones preferentially induced PS externalization ($P < 0.001$) in a dosedependent manner (Fig. 3a–b). Compared to 100 μM etoposide, which was used as a positive control, 25 μM dienone 2c was significantly more active in inducing apoptosis ($P < 0.001$; Fig. 3b). Untreated and solvent-treated cells did not exhibit any significant increment in apoptotic or necrotic values (Fig. 3a–b). These findings, which show that both 2b and 2c consistently induce PS externalization in MDA-MB-231 cells in a concentration-dependent manner, suggest that the mechanism underlying the cytotoxicity elicited by these dienones is apoptosis.

3.3 Dienone 2c induces mitochondrial depolarization

JC-1 is a useful reagent to identify cells undergoing mitochondrial depolarization ($\Delta\Psi m$), which is an early apoptotic event, indicated by emitting a green fluorescence signal that can be detected by flow cytometry [31]. In order to elucidate whether dienione 2c preferentially utilizes the mitochondrial/intrinsic pathway to induce cell death, MDA-MB-231 cells were incubated for 8 h as previously described [29]. By doing so, we found that cells exposed to dienone 2c (10 μM to 25 μM) exhibited a significant mitochondrial depolarization compared to solvent only or untreated control cells ($P < 0.001$; Fig. 4). These results indicate that dienone 2c induces $\Delta\Psi m$ perturbation in a concentration-dependent manner. Therefore, 2c appears to induce the intrinsic apoptotic pathway as a mechanism to inflict cell death.

3.4 Dienone 2c induces caspase-3 activation

In order to substantiate the above finding that mitochondrial depolarization is employed as an apoptosis-inducing pathway by dienone 2c, caspase-3 activation was assessed as a downstream apoptosis effector. To this end, MDA-MB-231 cells were exposed to dienone 2c

and subsequently incubated with a cell permeable NucView caspase-3 substrate, which permits live-cell detection of caspase-3 activation in single cells through flow cytometry. Cells exposed to dienone 2c (25 μM) exhibited significantly increased active caspase-3 values after a 8 h incubation period compared to untreated and solvent-only controls ($P < 0.001$; Fig. 5a), as previously instructed [32]. The percentages of cells with active caspase-3 increased ~9 fold after dienone 2c exposure from 10 μM to 25 μM ($P < 0.001$). These observations suggest that dienone 2c induces apoptosis via caspase-3 activation in MDA-MB-231 cells.

3.5 Dienone 2c elicits DNA fragmentation and cell cycle perturbation

To elucidate whether dienone 2c disturbs cell cycle progression in MDA-MB-231 cells, cell cycle analyses were carried out 48 h after treatment by flow cytometry. In addition, inter-nucleosomal DNA fragmentation, which occurs during late phases of apoptotic cell death, was detected through the presence of sub-G0/G1 cell populations. This method relies on a fluorescent DNA intercalating probe (DAPI) to quantify the nuclear DNA content. Low concentrations of dienone 2c were used to avoid massive cellular destruction. By doing so, we found that the sub-G0/G1 population encompassed 18.2 % of the cells exposed to 1 μM of dienone 2c, while at 3 μM this percentage increased to 43.85 % ($P < 0.001$; Fig. 6a, e, and f). Interestingly, the G0/G1, S and G2/M percentages were found to be significantly decreased ($P < 0.05$) in cells treated with 3 μM dienone 2c compared to those with 1 μM (Fig. 6b–d). The G2/M phase was less strongly affected by dienone 2c compared to the other cell cycle phases analyzed. Camptothecin-(4 μM) treated cells showed a slowdown of the rate of cell cycle progression, which was manifested by S phase arrest (38.2 %) without DNA fragmentation (Fig. 6a, c, and h). The percentages of cells in all phases of the cell cycle in DMSO treated (0.3 % *v*/*v*) and untreated cells were practically imperceptible (Figs. 6a–d, g, i), but significantly different from those in dienone 2c exposed cells ($P < 0.05$). Our results thus indicate that dienone 2c treated MDA-MB-231 cells exhibit apoptotic DNA fragmentation, predominantly related to diminished G0/G1 and S phase values in a dose-dependent manner ($P < 0.05$).

4 Discussion

Our results indicate that three curcumin analogues (dienones 2a-c) exhibit potent selective cytotoxic activity towards various human breast cancer-derived cells compared to non-malignant breast-derived cells. These dienones were more potent than the anti-cancer drug 5-FU. In addition, we found that dienones 2b and 2c exhibited higher selective cytotoxic indexes (SCI ranging from 18 to 150) to cancer cells compared to dienone 2a (SCI ranging from 24 to 45). No significant differences in cytotoxic potencies of the dienones were observed between non-metastatic MDA-MB-231 cells and its metastatic variant MDA-MB-231/LM2-4. Previously, dienones 2a and 2b were found to act as effective cytotoxins on human and mouse leukemia/lymphoma-derived cells [24]. Also, two other curcumin analogues were found to elicit cytotoxicity on MBA-MB-231 cells at sub-micromolar concentrations (CC_{50} of 0.8 and 0.3 μM, respectively). These analogues were, however, not compared to non-cancerous cells, thus preventing SCI determinations [33]. Moreover, demetho-xycurcumin (DMC), a natural curcuminoid, was found to show a selective toxic

effect on MDA-MB-231 cells with a CC_{50} slightly higher than 20 μM [34]. Therefore, dienone 2c is more effective in killing MDA-MB-231 cells with a higher SCI than DMC. Based on its high SCI and sub-micromolar CC_{50} concentrations, dienone 2c may serve as a potential anticancer drug. Here, we mainly focused on the biological activity and mechanism of action of dienone 2c, since the cytotoxic activities of dienones 2a and 2b have been reported before [24].

After exposure to a cytotoxic agent, cells may undergo necrosis or apoptosis. Apoptosis can be initiated by intrinsic or extrinsic biochemical pathways [35–37]. The intrinsic pathway mainly involves mitochondrial depolarization [35]. In order to substantiate our initial findings, several methods were used to determine the biochemical route by which the dienone analogues induce cell death. Our results indicated that the dienones 2b and 2c were able to induce PS externalization in MDA-MB-231 cells, rather than necrosis. PS externalization was more pronounced when the cells were exposed to higher concentrations of the dienones, indicating a dose-dependent tendency. To explore in more detail the molecular events underlying dienone 2c-induced cell death, its ability to elicit mitochondrial depolarization was assessed. Altered mitochondrial function may have profound effects on cell survival [38] due to an impairment of metabolic ATP production [39]. Mitochondrial-induced cell death includes dissipation of $\Delta\psi m$, which is known to activate the intrinsic apoptotic pathway [40]. Previously is was found that the synthetic polyphenol curcumin analog EF-24 provokes mitochondrial depolarization through $\Delta\Psi m$ in MDA-MB-231 cells [41]. Since we found that dienone 2c elicits PS translocation, MDA-MB-231 cells were exposed to dienone 2c after which $\Delta\Psi m$ was determined. Our results clearly showed that dienone 2c induced mitochondrial membrane depolarization in a dose-dependent manner, thus implicating the intrinsic apoptotic pathway as its mechanism of action.

Once a pro-apoptotic signal is inflicted upon a cell, a downstream cell death cascade will be activated. An intermediate biochemical event in this cascade is the activation of caspase-3 [42]. Caspase-3 is a converging enzyme of the main upstream intrinsic and extrinsic apoptotic pathways initiated by mitochondrial depolarization or death receptor activation, respectively [35]. Once caspase-3 is activated, apoptotic cell death is irreversible [43, 44]. Interestingly, it has previously been shown that curcumin induces concentration- and time-dependent caspase-3 activation in MDA-MB-231 cells [45]. To corroborate the induction of apoptosis by dienone 2c in our present study, caspase-3 activation was assessed. We found that caspase-3 was indeed activated in a concentration-dependent manner by dienone 2c, which is in agreement with our previous results indicating that this compound induces PS externalization and mitochondrial depolarization.

A well-established feature of apoptosis is the degradation of nuclear DNA via the activation of specific nucleases, such as caspase activated deoxiribonuclease (CAD) [46, 47]. DAPI-dsDNA complexes exhibit a fluorescence emission maximum at ~461 nm, whereas DAPI-RNA complexes exhibit a longer-wavelength emission maximum at ~500 nm [30]. Consequently, for the generation of high-resolution DNA content histograms, only the ~461 nm DAPI-dsDNA fluorescence emission signal was measured using a band pass filter that excluded the DAPI-RNA (~500 nm) emission signal [30]. This strategy allows DNA content analysis without the necessity to remove cellular RNA, which introduces significant noise in

the widely used PI method [14]. Additionally, this approach has the advantage of a faster sample processing time (~3 min), since it omits a lengthy cell fixation step and the removal of RNA by enzymatic digestion. By using this assay, dienone 2c was found to induce DNA fragmentation in MDA-MB-231 cells, as evidenced by increases in the sub-G0/G1 populations and reductions in the G0/G1 and S phase populations in a concentration-dependent manner without increases in the G2/M populations. Others have reported that EF-24 (a curcumin analogue) may cause a G2/M arrest in MDA-MB-231cells, suggesting that dienone 2c uses an alternative route [41].

Taken together, we show for the first time that dienone 2c exhibits cytotoxicity towards breast cancer-derived cells, including triple negative MDA-MB-231 cells. We found that dienone 2c induces phosphatidylserine externalization, mitochondrial depolarization, caspase-3 activation and DNA fragmentation, representing early, middle and late apoptotic events, respectively (Fig. 7). In addition, we found that dienone 2c was efficacious in killing both non-metastatic MDA-MB-231 cells and its metastatic variant at similar nanomolar concentrations. Dienone 2c has potential as a preclinical anti-breast cancer drug that preferentially induces apoptosis with a markedly high selective cytotoxicity towards breast cancer-derived cells. Dienone 2c has potential as an anti-breast cancer drug alone or in combination with standard anti-breast cancer chemotherapeutic drugs. Future *in vivo* work should lend support to its potential clinical use.

Acknowledgments

Funding for this work was provided by the National Institute of General Medical Sciences-Support of Competitive Research grant 1SC3GM103713-03 to RJA, as well as a Canadian Institutes of Health Research-Regional Partnerships Program Saskatchewan grant to JRD and UD. The authors also thank the Cytometry, Screening and Imaging Core Facility at the University of Texas at El Paso (UTEP), which was supported by a Research Centers in Minority Institutions program grant 2G12MD007592 to the Border Biomedical Research Center in UTEP from the National Institute on Minority Health and Health Disparities, a component of National Institutes of Health. The authors thank Gladys Almodovar and Sarah T. Baca (both with UTEP) for critical reviews of the manuscript and cell culture expertise, and to Drs. Karen Carr and John Norman (both with Beckman Coulter) for advice and instructions on the cell-cycle protocol, and also for the generous gift of the NIM-DAPI reagent. NMO, KP and ER-E were supported by NIGMS RISE training grant R25 GM069621-12. NMO was also supported by a Maximizing Access to Research Careers U*STAR program grant 2T34GM008048. KP was supported by the Student Mentoring to Achieve Retention: Triads in Science (SMARTS) program from National Science Foundation, grant DUE-1153832.

References

1. Howlader, N.; Noone, AM.; Krapcho, M.; Garshell, J.; Miller, D.; Altekruse, SF.; Kosary, CL.; Yu, M.; Ruhl, J.; Tatalovich, Z.; Mariotto, A.; Lewis, DR.; Chen, HS.; Feuer, EJ.; Cronin, KA. SEER Cancer Statistics Review, 1975-2012, National Cancer Institute. Bethesda, MD: http://seer.cancer.gov/csr/1975_2012/, based on November 2014 SEER data submission, posted to the SEER web site, April 2015. Accessed Jan 2016
2. Lu J, Steeg PS, Price JE, Krishnamurthy S, Mani SA, Reuben J, Cristofanilli M, Dontu G, Bidaut L, Valero V, Hortobagyi GN, Yu D. Breast cancer metastasis: challenges and opportunities. Cancer Res. 2009; 69:4951–4953. [PubMed: 19470768]
3. Cancer Genome Atlas Network. Comprehensive molecular portraits of human breast tumours. Nature. 2012; 490:61–70. doi:10. 1038/nature11412. [PubMed: 23000897]
4. Berardi DE, Flumian C, Campodonico PB, Urtreger AJ, Diaz Bessone MI, Motter AN, Bal de Kier Joffe ED, Farias EF, Todaro LB. Myoepithelial and luminal breast cancer cells exhibit different responses to all-trans retinoic acid. Cell. Oncol. 2015; 38:289–305. doi:10.1007/s13402-015-0230-z.

5. Fkih M'hamed I, Privat M, Ponelle F, Penault-Llorca F, Kenani A, Bignon YJ. Identification of miR-10b, miR-26a, miR-146a and miR-153 as potential triple-negative breast cancer bio-1markers. Cell. Oncol. 2015; 38:433–442. doi:10.1007/s13402-015-0239-3.
6. Moelans CB, Vlug EJ, Ercan C, Bult P, Buerger H, Cserni G, van Diest PJ, Derksen PW. Methylation biomarkers for pleomorphic lobular breast cancer - a short report. Cell. Oncol. 2015; 38:397–405. doi:10.1007/s13402-015-0241-9.
7. You Y, Li H, Qin X, Zhang Y, Song W, Ran Y, Gao F. Decreased CDK10 expression correlates with lymph node metastasis and predicts poor outcome in breast cancer patients - a short report. Cell. Oncol. 2015; 38:485–491. doi:10.1007/s13402-015-0246-4.
8. Vargo-Gogola T, Rosen JM. Modelling breast cancer: one size does not fit all. Nat. Rev. Cance. 2007; 7:659–672.
9. Dent R, Trudeau M, Pritchard KI, Hanna WM, Kahn HK, Sawka CA, Lickley LA, Rawlinson E, Sun P, Narod SA. Triple-negative breast cancer: clinical features and patterns of recurrence. Clin. Cancer Res. 2007; 13:4429–4434. [PubMed: 17671126]
10. Badve S, Dabbs DJ, Schnitt SJ, Baehner FL, Decker T, Eusebi V, Fox SB, Ichihara S, Jacquemier J, Lakhani SR, Palacios J, Rakha EA, Richardson AL, Schmitt FC, Tan P-H, Tse GM, Weigelt B, Ellis IO, Reis-Filho JS. Basal-like and triple-negative breast cancers: a critical review with an emphasis on the implications for pathologists and oncologists. Mod. Pathol. 2011; 24:157–167. [PubMed: 21076464]
11. Cailleau R, Young R, Olive M, Reeves WJ Jr. Breast tumor cell lines from pleural effusions. J. Natl. Cancer Inst. 1974; 53:661–674. [PubMed: 4412247]
12. Munoz R, Man S, Shaked Y, Lee CR, Wong J, Francia G, Kerbel RS. Highly efficacious nontoxic preclinical treatment for advanced metastatic breast cancer using combination oral UFT-cyclophosphamide metronomic chemotherapy. Cancer Res. 2006; 66:3386–3391. [PubMed: 16585158]
13. Soule HD, Maloney TM, Wolman SR, Peterson WD Jr. Brenz R, McGrath CM, Russo J, Pauley RJ, Jones RF, Brooks SC. Isolation and characterization of a spontaneously immortalized human breast epithelial cell line, MCF-10. Cancer Res. 1990; 50:6075–6086. [PubMed: 1975513]
14. Robles-Escajeda E, Martinez A, Varela-Ramirez A, Sanchez-Delgado RA, Aguilera RJ. Analysis of the cytotoxic effects of ruthenium-ketoconazole and ruthenium-clotrimazole complexes on cancer cells. Cell Biol. Toxicol. 2013; 29:431–443. [PubMed: 24272524]
15. Mohankumar K, Pajaniradje S, Sridharan S, Singh VK, Ronsard L, Banerjea AC, Selvanesan BC, Coumar MS, Periyasamy L, Rajagopalan R. Apoptosis induction by an analog of curcumin (BDMC-A) in human laryngeal carcinoma cells through intrinsic and extrinsic pathways. Cell. Oncol. 2014; 37:439–454. doi:10.1007/s13402-014-0207-3.
16. Pereira MA, Grubbs CJ, Barnes LH, Li H, Olson GR, Eto I, Juliana M, Whitaker LM, Kelloff GJ, Steele VE, Lubet RA. Effects of the phytochemicals, curcumin and quercetin, upon azoxymethane-induced colon cancer and 7, 12-dimethylbenz[a]anthracene-induced mammary cancer in rats. Carcinogenesis. 1996; 17:1305–1311. [PubMed: 8681447]
17. Rao TS, Basu N, Siddiqui HH. Anti-inflammatory activity of curcumin analogues. Indian J. Med. Res. 1982; 75:574–578. [PubMed: 7118227]
18. Mutus B, Wagner JD, Talpas CJ, Dimmock JR, Phillips OA, Reid RS. 1-p-Chlorophenyl-4,4-dimethyl-5-diethylamino-1-penten-3-one hydrobromide, a sulfhydryl-specific compound which reacts irreversibly with protein thiols but reversibly with small molecular weight thiols. Anal. Biochem. 1989; 177:237–243. [PubMed: 2729541]
19. Page, CP. Integrated pharmacology. 3rd. Elsevier Mosby; Edinburgh: 2006.
20. Das U, Sharma RK, Dimmock JR. 1,5-diaryl-3-oxo-1,4-pentadienes: a case for antineoplastics with multiple targets. Curr. Med. Chem. 2009; 16:2001–2020. [PubMed: 19519378]
21. Chen G, Waxman DJ. Role of cellular glutathione and glutathione S-transferase in the expression of alkylating agent cytotoxicity in human breast cancer cells. Biochem. Pharmacol. 1994; 47:1079–1087. [PubMed: 8147907]
22. Mitchell JB, Russo A. The role of glutathione in radiation and drug induced cytotoxicity. Br. J. Cancer Suppl. 1987; 8:96–104. [PubMed: 3307879]

23. Dimmock JR, Padmanilayam MP, Puthucode RN, Nazarali AJ, Motaganahalli NL, Zello GA, Quail JW, Oloo EO, Kraatz HB, Prisciak JS, Allen TM, Santos CL, Balzarini J, De Clercq E, Manavathu EK. A conformational and structure-activity relationship study of cytotoxic 3,5-bis(arylidene)-4-piperidones and related N-acryloyl analogues. J. Med. Chem. 2001; 44:586–593. [PubMed: 11170648]
24. Das U, Alcorn J, Shrivastav A, Sharma RK, De Clercq E, Balzarini J, Dimmock JR. Design, synthesis and cytotoxic properties of novel 1-[4-(2-alkylaminoethoxy)phenylcarbonyl]-3,5-bis(arylidene)-4-piperidones and related compounds. Eur. J. Med. Chem. 2007; 42:71–80. [PubMed: 16996657]
25. Lema C, Varela-Ramirez A, Aguilera RJ. Differential nuclear staining assay for high-throughput screening to identify cytotoxic compounds. Curr Cell. Biochem. 2011; 1:1–14. [PubMed: 27042697]
26. Debnath J, Muthuswamy SK, Brugge JS. Morphogenesis and oncogenesis of MCF-10A mammary epithelial acini grown in three-dimensional basement membrane cultures. Methods. 2003; 30:256–268. [PubMed: 12798140]
27. Nunes LM, Robles-Escajeda E, Santiago-Vazquez Y, Ortega NM, Lema C, Muro A, Almodovar G, Das U, Das S, Dimmock JR, Aguilera RJ, Varela-Ramirez A. The gender of cell lines matters when screening for novel anti-cancer drugs. AAPS J. 2014; 16:872–874. [PubMed: 24875051]
28. Varela-Ramirez A, Costanzo M, Carrasco YP, Pannell KH, Aguilera RJ. Cytotoxic effects of two organotin compounds and their mode of inflicting cell death on four mammalian cancer cells. Cell Biol. Toxicol. 2011; 27:159–168. [PubMed: 21069563]
29. Robles-Escajeda E, Lerma D, Nyakeriga AM, Ross JA, Kirken RA, Aguilera RJ, Varela-Ramirez A. Searching in mother nature for anti-cancer activity: anti-proliferative and pro-apoptotic effect elicited by green barley on leukemia/lymphoma cells. PLoS One. 2013; 8:e73508. [PubMed: 24039967]
30. Valdez, B.; Carr, K.; Norman, J. Beckman Coulter Life Sciences. Houston, TX: Violet-excited nim-DAPI allows efficient and reproducible cell cycle analysis on the Gallios flow cytometer. http://www.bcilifesciences.com/flow/DAPIwhitepaper/BR-18940.pdf. Accesed Jan 2016
31. Li H, Zhu H, Xu CJ, Yuan J. Cleavage of BID by caspase 8 mediates the mitochondrial damage in the Fas pathway of apoptosis. Cell. 1998; 94:491–501. [PubMed: 9727492]
32. Pedroza DA, De Leon F, Varela-Ramirez A, Lema C, Aguilera RJ, Mito S. The cytotoxic effect of 2-acylated-1,4-naphthohydroquinones on leukemia/lymphoma cells. Biorg. Med. Chem. 2014; 22:842–847. doi:10.1016/j.bmc.2013.12.007.
33. Yadav B, Taurin S, Rosengren RJ, Schumacher M, Diederich M, Somers-Edgar TJ, Larsen L. Synthesis and cytotoxic potential of heterocyclic cyclohexanone analogues of curcumin. Biorg. Med. Chem. 2010; 18:6701–6707.
34. Shieh J-M, Chen Y-C, Lin Y-C, Lin J-N, Chen W-C, Chen Y-Y, Ho C-T, Way T-D. Demethoxycurcumin inhibits energy metabolic and oncogenic signaling pathways through AMPK activation in triple-negative breast cancer cells. J. Agric. Food Chem. 2013; 61:6366–6375. [PubMed: 23777448]
35. Solary E, Droin N, Bettaieb A, Corcos L, Dimanche-Boitrel MT, Garrido C. Positive and negative regulation of apoptotic pathways by cytotoxic agents in hematological malignancies. Leukemia. 2000; 14:1833–1849. [PubMed: 11021759]
36. Birsu Cincin Z, Unlu M, Kiran B, Sinem Bireller E, Baran Y, Cakmakoglu B. Anti-proliferative, apoptotic and signal transduction effects of hesperidin in non-small cell lung cancer cells. Cell. Oncol. 2015; 38:195–204. doi:10.1007/s13402-015-0222-z.
37. Nakaoka T, Ota A, Ono T, Karnan S, Konishi H, Furuhashi A, Ohmura Y, Yamada Y, Hosokawa Y, Kazaoka Y. Combined arsenic trioxide-cisplatin treatment enhances apoptosis in oral squamous cell carcinoma cells. Cell. Oncol. 2014; 37:119–129. doi:10.1007/s13402-014-0167-7.
38. Loeb LA, Wallace DC, Martin GM. The mitochondrial theory of aging and its relationship to reactive oxygen species damage and somatic mtDNA mutations. PNAS. 2005; 102:18769–18770. [PubMed: 16365283]
39. Westermann B. Mitochondrial fusion and fission in cell life and death. Nat. Rev. Mol. Cell Biol. 2010; 11:872–884. [PubMed: 21102612]

40. Lahouel M, Amedah S, Zellagui A, Touil A, Rhouati S, Benyache F, Leghouchi E, Bousseboua H. The interaction of new plant flavonoids with rat liver mitochondria: relation between the anti- and pro-oxydant effect and flavonoids concentration. Therapie. 2006; 61:347–355. [PubMed: 17124951]

41. Adams BK, Cai J, Armstrong J, Herold M, Lu YJ, Sun A, Snyder JP, Liotta DC, Jones DP, Shoji M. EF24, a novel synthetic curcumin analog, induces apoptosis in cancer cells via a redox-dependent mechanism. Anticancer Drugs. 2005; 16:263–275. [PubMed: 15711178]

42. Igney FH, Krammer PH. Death and anti-death: tumour resistance to apoptosis. Nat. Rev. Cancer. 2002; 2:277–288. [PubMed: 12001989]

43. Kothakota S, Azuma T, Reinhard C, Klippel A, Tang J, Chu K, McGarry TJ, Kirschner MW, Koths K, Kwiatkowski DJ, Williams LT. Caspase-3-generated fragment of gelsolin: effector of morphological change in apoptosis. Science. 1997; 278:294–298. [PubMed: 9323209]

44. Ly JD, Grubb DR, Lawen A. The mitochondrial membrane potential (deltapsi(m)) in apoptosis; an update. Apoptosis. 2003; 8:115–128. [PubMed: 12766472]

45. Gogada R, Amadori M, Zhang H, Jones A, Verone A, Pitarresi J, Jandhyam S, Prabhu V, Black JD, Chandra D. Curcumin induces Apaf-1-dependent, p21-mediated caspase activation and apoptosis. Cell Cycle. 2011; 10:4128–4137. doi:10. 4161/cc.10.23.18292. [PubMed: 22101335]

46. Fadeel B, Orrenius S, Zhivotovsky B. Apoptosis in human disease: a new skin for the old ceremony? Biochem. Biophys. Res. Commun. 1999; 266:699–717. doi:10.1006/bbrc.1999.1888.

47. Nagata S. Apoptotic DNA fragmentation. Exp. Cell Res. 2000; 256:12–18. [PubMed: 10739646]

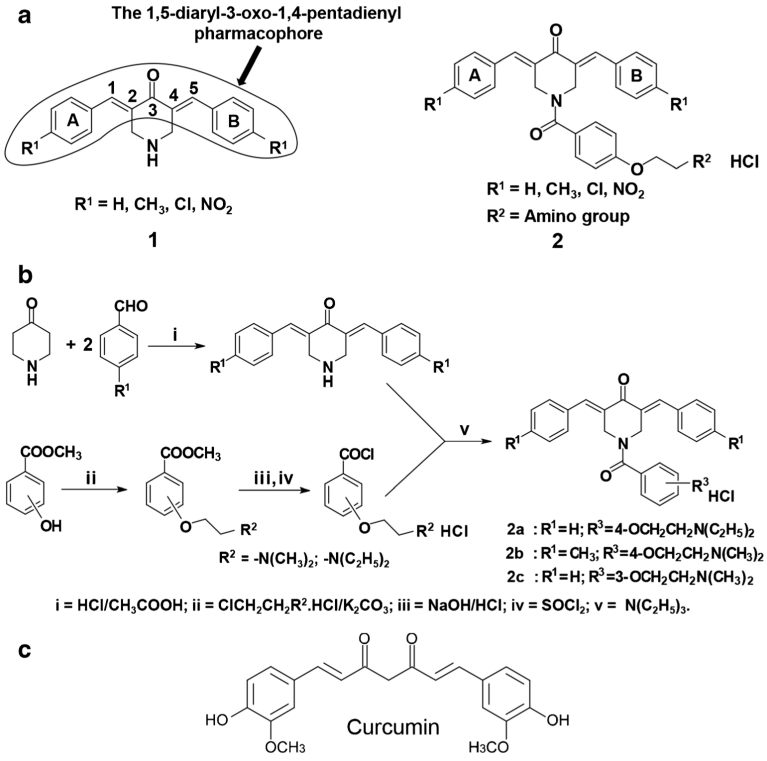

Fig. 1.

a General structures of series 1 and 2 of cytotoxins containing the 1,5-diaryl-3-oxo-1,4-pentadienyl pharmacophore. **b** Synthesis of 3,5-bis(benzylidene)-1-[4-(2-diethylaminoethyloxy) phenylcarbonyl]-4-piperidone hydrochloride hemihydrate, dienone 2a, 1-[4-(2-dimethylaminoethoxy)phenylcarbonyl]-3,5-bis(4-methylbenzylidene)-4-piperidone hydrochloride hemihydrate, dienone 2b and 3,5-bis(benzylidene)-1-[3-(2-dimethylaminoethoxy)phenylcarbonyl]-4-piperidone hydrochloride, dienone 2c. c Structure of curcumin

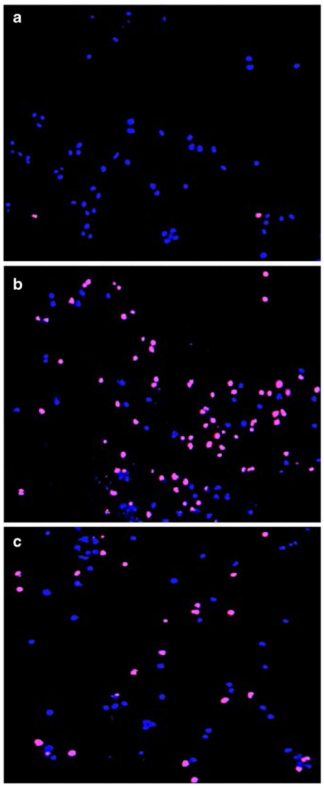

Fig. 2.

Representative overlay of live-cell images of MB-231 cells stained with Hoechst and propidium iodide (PI) used to determine CC_{50} values. (**a**) Nuclei of untreated cells that serve as a negative control. (**b**) Cells treated with the pro-apoptotic agent H_2O_2 (100 μM), resulted in a significant increase in PI-positive cells (dying cells; magenta color due to overlay of blue and red dyes). (**c**) Cells treated with dienone 2c (0.8 μM) displaying an increase in dying cells as in (**b**). Nuclei exhibiting a blue signal only are considered to be living cells

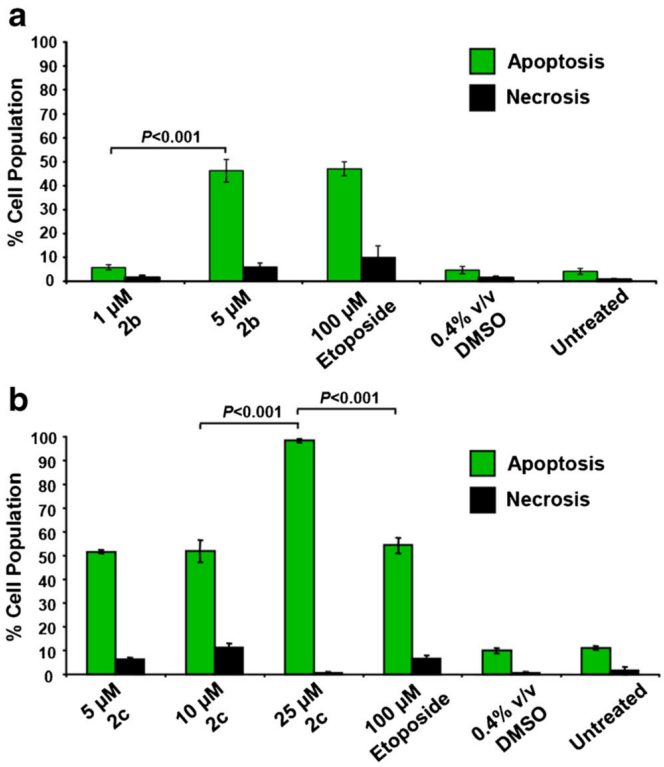

Fig. 3.

Dienones 2b and 2c induce PS externalization in a concentration-dependent manner in MDA-MB-231 cells after a 48 h treatment. PS externalization was measured by flow cytometry. The total percentages of apoptotic cells (*y*-axis) are expressed as the sum of the percentages of early and late stages of apoptosis (*green bars*), as determined by the percentage of annexin V-FITC positive cells. (**a** and **b**) Cells exposed to the dienones that were only PI positive are considered to be necrotic (*black bars*). Each bar represents the average of three independent measurements and the *error bars* represent their corresponding standard deviations. The following controls were included: cells exposed to 100 μM etoposide as a positive control for apoptosis; cells treated with 0.4 % *v*/*v* DMSO as a solvent control; untreated cells as a negative control. Approximately 3000 events (cells) were collected and analyzed per sample using CXP software (Beckman Coulter)

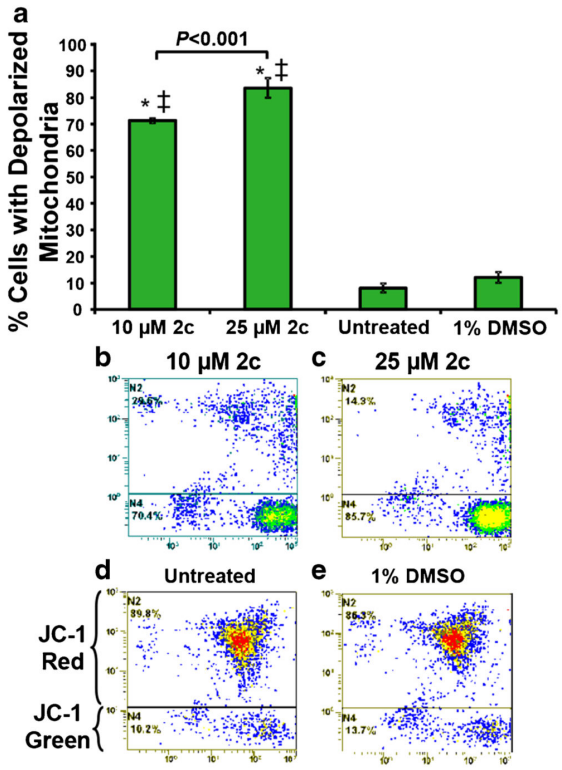

Fig. 4.

The cytotoxicity of dienone 2c is mediated by $\Delta\Psi m$ changes in MDA-MB-231 cells in a dose-dependent manner. After 8 h of treatment with 10 and 25 μM dienone 2c, changes in $\Delta\Psi m$ were monitored by JC-1 staining and flow cytometry. Dissipation of $\Delta\Psi m$ causes the JC-1 reagent to emit a green fluorescence signal, and a red signal when mitochondrial membranes are polarized. The average percentages of cells with depolarized membranes are shown in (**a**). Untreated and 1 % DMSO (0.4 % *v*/*v*) treated cells were used as controls. Statistical significance was determined using the two-tailed Student's paired t-test of dienone 2c treated with untreated (*) and DMSO treated cells (‡). $P < 0.001$. Representative flow cytometric dot plots used to determine the percentages of cells with depolarized mitochondria are depicted in panels **b**–**e**

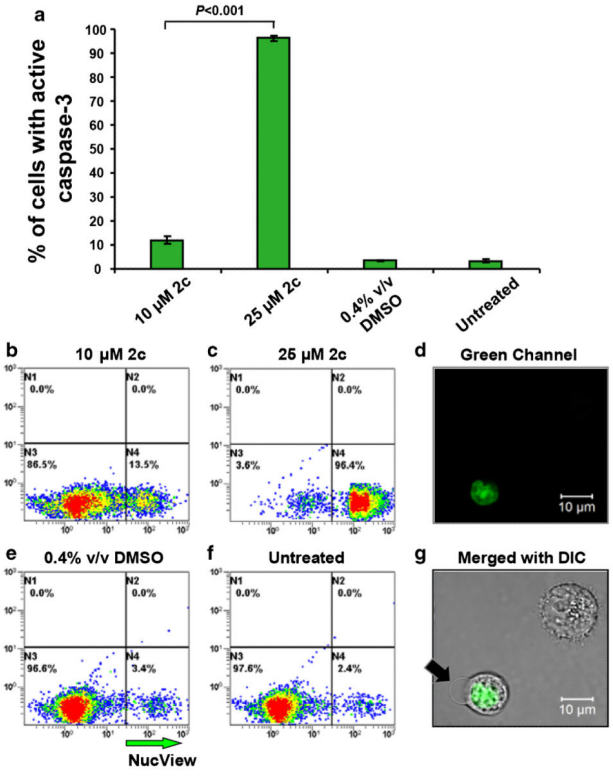

Fig. 5.

Dienone 2c induces caspase-3 activation in a concentration-dependent manner in MDA-MB-231 cells. Intracellular active caspase-3 was detected after a 8 h incubation with dienone 2c using a NucView 488 fluorogenic substrate in conjunction with flow cytometry. The percentage of active caspase 3-positive cells, exhibiting a green fluorescence signal, are indicated on the y-axis, whereas on the x-axis the different treatments are indicated (**a**). Each bar represents the average of three independent measurements, and error bars correspond to the standard deviation of the mean. Representative *dot* plots used to obtain the percentages of cells positive to the NucView caspase-3/7 substrate are indicated on the y-axis (FL2 detector), whereas the FL1 detector measurements are depicted on the x-axis (**b**–**f**). After exposure to 10 μM (**b**) and 25 μM (**c**) dienone 2c for 8 h, the cells were incubated with the caspase-3 substrate, as detailed in Material and Methods. Solvent control (0.4 % DMSO; e) and untreated cells (**f**) were included as controls. Approximately 10,000 events were collected and analyzed per sample using CXP software (Beckman Coulter). Images of a representative cell captured in the green fluorescence channel (**d**) and the merged image of both the green and the differential interference contrast (DIC) channels (**g**) are depicted. In the merged image (**g**), the *black arrow* indicates the presence of a bleb, a morphological feature of apoptosis. The top right cell is negative for the NucView caspase-3/7 substrate

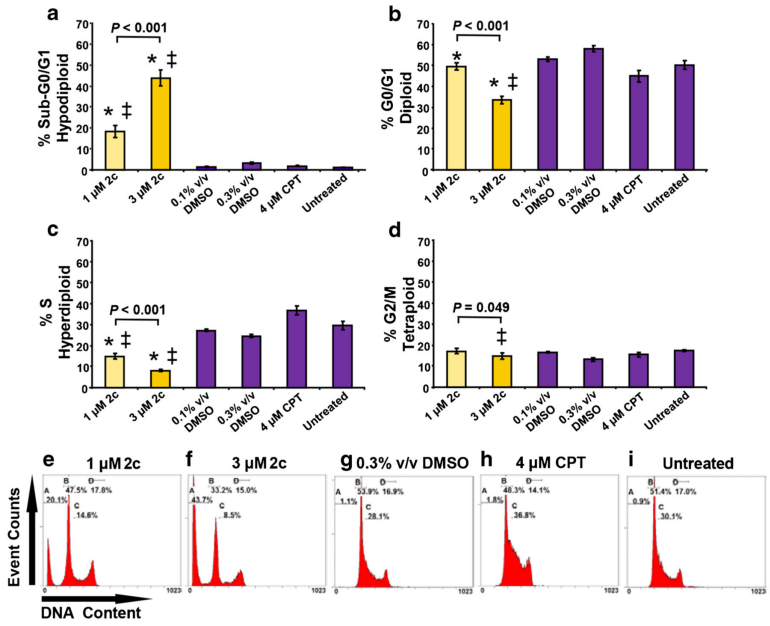

Fig. 6.

Dienone 2c disturbs the cell cycle profile of breast cancer-derived cells and induces DNA fragmentation associated with reduced G0/G1 and S phase values in a dose-dependent manner. Cells were harvested, permeabilized, DAPI stained and analyzed by flow cytometry. (a–d) The percentages of cells in each phase are plotted along the y-axis and the different treatments are graphed along the x-axis. Each bar represents the average of four independent replicates, and the error bars represent the corresponding standard deviations. Several controls were included (purple bars): solvent controls (0.1 or 0.3 % *v*/*v* DMSO), a reference drug (4 μM camptothecin, CPT) and untreated cells. Significant differences between 1 and 3 μM dienone 2c treated cells compared to their corresponding 0.1 % or 0.3 % *v*/*v* DMSO treated cells (*) and untreated cells (‡) were $P < 0.05$. (e–i) Representative flow cytometric histograms employed to quantify the distributions of the cell cycle phases. Gates in the flow cytometric histograms (panels e–i) are from left to right: sub-G0/G1 (hypodiploid; counted as apoptotic subpopulation), G0/G1 (diploid), S (hyperdiploid) and G2/M (tetraploid)

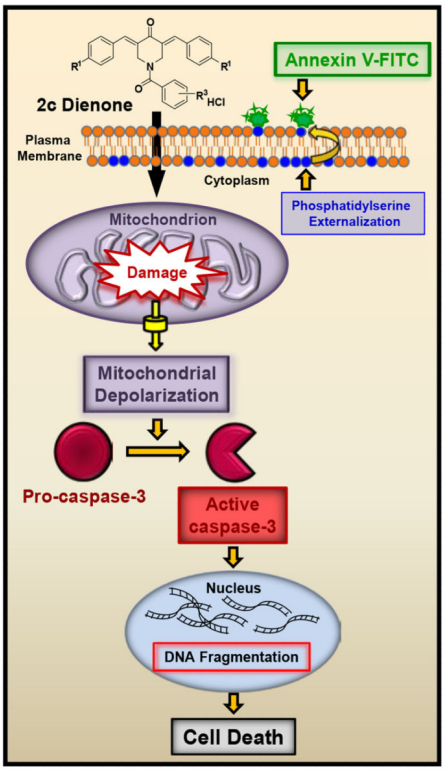

Fig. 7.

Schematic diagram depicting the suggested mechanisms involved in dienone 2c-induced apoptosis in MDA-M B-231 cells. Dienone 2c elicits the following pro-apoptotic biochemical phases: phosphatidylserine externalization, mitochondrial depolarization, caspase-3 activation, DNA fragmentation and cell death, which are indicative of early, middle and late apoptotic stages, respectively

Table 1

Cytotoxic concentration 50% (CC_{50}) and selective cytotoxicity index (SCI) values of experimental compounds obtained after 72 h exposure of several breast-derived cell lines

Cell Line	2a	2b	2c	5-FU[a]
MDA-MB-231	0.91[b] (45[c])	0.72 (111)	0.88 (90)	7.85
MDA-MB-231-LM	0.90 (45)	0.53 (150)	1.11 (71)	6.03
HCC1419	1.67 (24)	1.7 (47)	1.46 (54)	>10[d]
MCF-7	1.64 (25)	4.4 (18)	1.83 (43)	1.7
MCF-10A	41.03	80.02	79.65	N/D

N/D not determined

[a] 5-Fluorouracil (5-FU) was used as a reference drug

[b] Cytotoxic concentration 50% (in μM) is defined as the concentration of drug required to disrupt the integrity of the cellular membrane of 50% of the cell population compared to DMSO treated cells, after 72 h of incubation as determined by the DNS assay

[c] The selective cytotoxicity index (SCI)

[d] The CC_{50} for 5-FU could not be determined for this cell line since the highest concentration tested (10 μM) resulted in only 3 % cell death